applied sciences

MDPI

Article

Investigating the Threshold Conditions of Air Breakdown with Mode-Locked Q-Switched Laser Pulses, and the Temporal Dynamics of Induced Plasma with Self-Scattering Phenomenon

Kai-Ting Yen [1], Chih-Hung Wu [1], Pin-Hsun Wang [1], Pi-Hui Tuan [2] and Kuan-Wei Su [1,*]

[1] Department of Electrophysics, National Yang Ming Chiao Tung University, 1001 Ta-Hsueh Rd., Hsinchu 30010, Taiwan; df900035.sc06@nycu.edu.tw (K.-T.Y.); tingyih@hotmail.com (C.-H.W.); simon0752059.ep07g@nctu.edu.tw (P.-H.W.)

[2] Department of Physics, National Chung Cheng University, 168 University Rd., Minhsiung, Chiayi 621301, Taiwan; phtuan@ccu.edu.tw

* Correspondence: sukuanwei@nycu.edu.tw

Abstract: A Q-switched Nd:YAG laser with mode-locked modulations is utilized to explore the laser-induced air breakdown. The various modulation depths of the mode-locking within the Q-switched pulse can be utilized to investigate the threshold conditions. With the GHz high-speed detectors to accurately measure the temporal pulse shape pulse by pulse, it is verified that the air breakdown threshold is crucially determined by the peak-power density instead of the energy density from the statistic results, especially for mode-locked Q-switched lasers. The stability of the system for laser-induced breakdown can be evaluated by threshold width through fitting the statistical result. Otherwise, by measuring the temporal characteristics of the excitation pulse and the induced plasma, it is further found that the plasma radiation displays a few-nanoseconds time delay to the excitation pulse and shows a decaying tail to be 10 times longer than the plasma build-up time. Moreover, the incident laser pulse is observed to be self-scattered by the air breakdown, and a rapidly modulated scattering rate is found with a slight delay time to the excitation mode-locked subpulse modulations.

Keywords: laser-induced breakdown; solid-state lasers; plasma dynamics

Citation: Yen, K.-T.; Wu, C.-H.; Wang, P.-H.; Tuan, P.-H.; Su, K.-W. Investigating the Threshold Conditions of Air Breakdown with Mode-Locked Q-Switched Laser Pulses, and the Temporal Dynamics of Induced Plasma with Self-Scattering Phenomenon. *Appl. Sci.* **2022**, *12*, 41. https://doi.org/10.3390/app12010041

Academic Editors: Bernhard Wilhelm Roth and Edik U. Rafailov

Received: 20 October 2021
Accepted: 15 December 2021
Published: 21 December 2021

1. Introduction

Gas breakdowns generated by high-power optical pulses can be traced back to the groundbreaking era for lasers [1,2]. Since then, the technologies of laser-induced breakdowns (LIBs) have been intensely studied and developed to be mature applications, including laser ablation [3], micromachining [4], photochemistry [5], laser fusion [6], laser-induced breakdown spectroscopy [7], laser ignition [8,9], and cavitation bubble generation [10]. The LIB is generally described as the formation of ionized gas or plasma during or by the end of the excitation of the laser pulse. Physically, the breakdown and ionization of the gas molecules are triggered when the electric field of the laser pulse is greater than that of the binding electrons to their nuclei [11]. After the initial breakdown, the avalanche ionization through some cascade effects takes place to vastly increase the plasma density of the gas molecules [12,13]. In addition to the gas breakdown, the interaction between ns laser and matter was deeply studied [14,15]. Since LIB belongs to a threshold-like process with respect to the peak intensity of the laser pulse [16–18], determining the breakdown threshold has long been a critical issue for reliable results of the developed applications.

In general, the threshold criterion for LIB is defined by the minimum laser energies at which 10–50% of the laser firings result in an observable optical breakdown [11,19–21]. A few reports also propose that it is adequate to determine the breakdown threshold by the laser power intensity for taking the focused laser beam radius into account [18,22,23]. The thresholds of LIBs under different experimental conditions—such as laser wavelengths [24], pulse durations [25], gas pressures [26], compositions of gas molecules [27], and focal

point properties [28,29]—have been widely investigated. Due to the limitation of the response time of photodetectors, the temporal shapes of laser pulses were usually assumed to have Gaussian-like profiles for calculating the breakdown intensities in most works of literature [19,20]. We call these laser pulses the pure Q-switched laser pulses. However, most of the temporal shapes of pure Q-switched pulse still have some small sub-pulse modulations by mode beating or slightly mode-locking that might not have been noticed for LIB in the past. In recent years, researchers have started to study the science of air-breakdown plasma using such modulated Q-switched pulse [23]. Moreover, because the actual temporal profiles of laser were not explicitly resolved and monitored pulse-by-pulse, the determined threshold intensities may have large fluctuations even under similar experimental arrangements [30,31]. Thanks to the development of high-speed optical detecting technologies, the high-resolution temporal behaviors of laser pulses can be precisely measured. This improvement enables us to resolve the temporal dynamics further to find out the most crucial threshold condition for the initial breakdown.

In this work, we utilized the lamp-pumped high-energy Q-switched Nd:YAG laser to explore the threshold conditions of the air breakdown. Based on the designed convex-concave resonator for good beam quality [32] and wedged gain crystal to avoid etalon effect for simultaneously mode-locking [33,34]. The mode-locking modulation may have suffered from the instabilities caused by the inhomogeneous thermal loading and cavity misalignment [35,36]. By utilizing this feature, we can generate laser pulses with various temporal shapes to study the influences of peak-power intensity on the gas breakdown. Both qualitative observation and the statistics results indicated that the breakdown threshold was determined mainly by the peak-power intensity instead of the pulse energy density. The threshold of peak-power intensity for air breakdown was found to be 0.63 TW / cm^2. The threshold width was also determined through a phenomenological formula. On the other hand, pulse lasers with lower energy breakdown thresholds are more suitable for ophthalmology surgery [37] and microfluidics [38]. This work shows that the energy breakdown threshold of deeply-mode-locked Q-switched pulse was 0.36 times lower than pure Q-switched pulse.

In addition, with sub-nanosecond mode-locked subpulses, we studied the temporal dynamics of incident laser, residual laser, scattered laser, and radiation of induced plasma. Part of the following incident laser photons was scattered by the plasma induced by the same incident laser pulse itself. The time-dependent self-scattering rate of plasma was obtained without additional probe light, and showed the fast response to the mode-locked subpulses. The observation may inspire further study on fine-structured plasma formation for aerospace science and point scattering for 3D display in mid-air. Finally, the time-averaged radiation spectrum of the induced plasma was measured and confirmed to correspond well to the excited levels of the composite molecules in air [39].

2. Experimental Setup

The schematic diagram for the experimental setup is shown in Figure 1. A Xe flash lamp with an arc length of 70 mm, normal pressure 450 Torr, and a maximum energy output of 20 J at 850 volts was used as the pump source. A 1.1 at %-doped Nd:YAG rod with a length of 50 mm and a diameter in 3 mm was used as the gain medium. Both surfaces of the gain medium were coated with anti-reflection (AR, $R < 0.01\%$) at 1064 nm and wedged with 2 degrees to prevent the parasitic pulse and the unwanted etalon effect. The Nd:YAG rod and the flash lamp were placed inside a pumping enclosure consisting of reflectors coated with silver on the inside surface to improve the pump efficiency. The laser resonator was designed as a convex-concave cavity to enlarge the laser mode volume for achieving high pulse-energy output with good beam quality [32]. The radius of curvature of the convex front mirror was -500 mm, and the surface was coated for high reflection (HR, $R > 99.9\%$) at 1064 nm. For the concave output coupler, the radius of curvature for the resonant surface was 600 mm, and the coating was partially reflective ($R = 55\%$) at 1064 nm. The 1064 nm anti-reflective coated outer surface of the output coupler was designed to be convex with a

curvature of −140 mm to reduce the output divergence. A Cr^{4+}:YAG crystal with initial transmittance of 35% was employed as the saturable absorber. The effective cavity length was chosen to be 90 mm. With a weak thermal lensing effect, the laser was operated in a stable region [32,34]. The output pulse energy was able to be stabilized around 21 mJ with one-sigma stability of 1% under continuous-firing operation at a repetition rate of 0.2 Hz after warm-up. However, under the randomly single-shot operation, the one-sigma energy stability was up to 3%, coinciding with an increased energy fluctuation of ±10%. For varied incident energy for the air breakdown, an attenuator was placed behind the laser cavity to adjust the pulse energy by utilizing the polarization given by the Brewster plate. The Q-switched pulses were able to be attenuated with a range from 0 to 11 mJ.

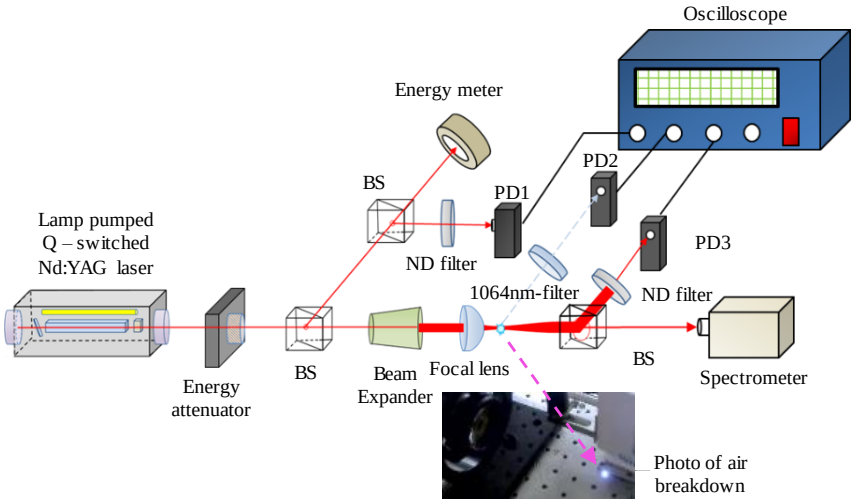

Figure 1. Schematic diagram of experimental setup and the photo of air breakdown. BS: beam splitter; PD: photodetector.

A focusing unit composed of a beam expander with 10 times magnification and a triplet focusing lens with a 12 cm focal length is exploited to tightly focus the Q-switched pulses for inducing breakdown in atmospheric air. The focused laser beam waist of 7 µm in radius was measured through the knife-edge method. We also measured the beam radius within 1–3 mm before and after the focal point to verify the beam size at focal point through the curve fitting with Gaussian-beam propagation theory. High-speed photodetectors with a silicon base (PD2, EOT Inc., ET-2030 with rising time 300 ps) and an InGaAs base (PD1, PD3, EOT Inc. (Traverse City, MI, USA), ET-3500 with rising time 25 ps) were respectively employed to detect the temporal characteristics of the induced plasma as well as the incident and residual laser pulses. The output signal of the photodetectors was connected to a digital oscilloscope (Agilent DSO 80,000) with 10 GHz electrical bandwidth and a sampling interval of 25 ps. The time-averaged radiation spectrum of the induced plasma is measured by a compact spectrometer (UVisIR Inc. (Traverse City, MI, USA), FullScan-LR) with a resolution < 5 nm.

3. Results

3.1. Qualitative Observation of the Threshold Conditions

First, we use another slightly degraded laser cavity with larger instability, then single shot randomly without warm-up. Figure 2 shows the output pulses with various temporal profiles in the test range from 2.9 to 3.4 mJ while the attenuation ratio of the attenuator was fixed. In most pulses, the modulations originated from the mode-locking mechanism can be clearly seen since the unwanted etalon effect was prevented [40]. It can also be found that, with deeper modulations, the pulses under nearly the same pulse energy will possess higher peak power, such as the comparisons between Figure 2b,c as well as Figure 2d,e. After firing hundreds of pulses, we found that all the pulses like Figure 2b,d

cannot induce air breakdown. On the contrary, all the pulses like Figure 2c,e can induce air breakdown. By using mode-locked Q-switched pulses, the qualitative observation implied that the peak power could dominate the threshold condition of air breakdown. In the forthcoming section, the threshold conditions were investigated through a quantitative method to support this observation.

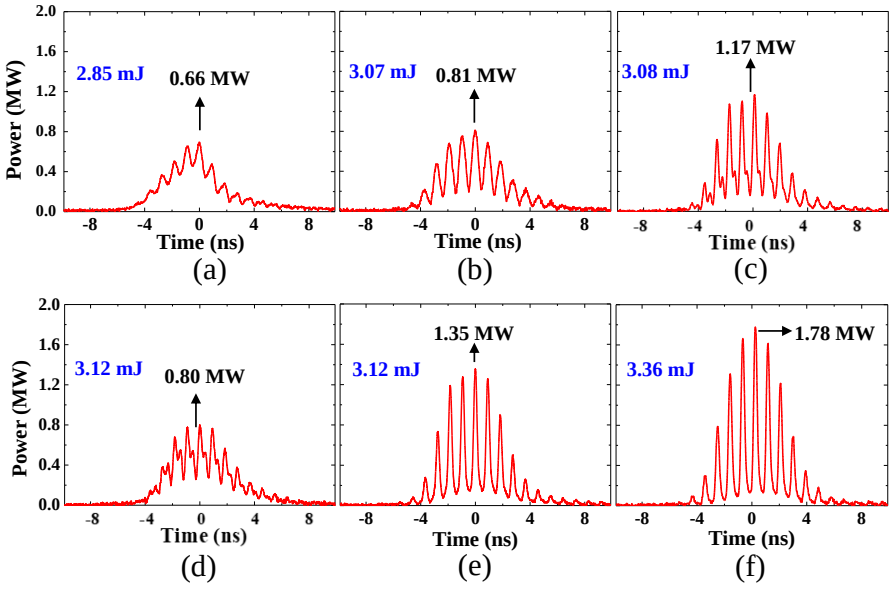

Figure 2. (**a**–**f**) Mode-locked Q-switched pulses with various temporal profiles in the test energy range from 2.9 to 3.4 mJ.

3.2. A Statistic Method to Evaluate the Threshold and Investigate the Threshold Conditions

In order to determine the threshold of peak-power intensity and energy density for the initial breakdown under continuous-firing operation at a repetition rate of 0.2 Hz after warm-up, hundreds of mode-locked Q-switched (ML-QS) pulses were tightly focused into the atmospheric air. Note that the temporal profiles of these laser pulses have been monitored pulse-by-pulse to determine the region of threshold fairly. The pulse width of the envelope of ML-QS pulses was 7 ns on average. Figure 3a shows the relation of the successes of air breakdowns to the laser energy and laser peak power with ML-QS laser. The experimental results indicate that the success of the initial breakdown is slightly related to the pulse energy but mainly dominated by the peak power in the energy range from 2.10 to 3.05 mJ, corresponding to an energy density range from 1.36 to 1.98 kJ / cm^2. To analyze the influence of peak power on air breakdown for the specific laser cavity more explicitly, the statistics on the breakdown probability, ρ, with respect to the peak power, P, was performed in Figure 3b. For determining the threshold peak power, P_{th}, threshold width of peak power, ΔP, and normalized threshold width of peak power, $\Delta\widetilde{P}$, a phenomenological formula was used to fit the experimental data numerically as

$$\rho(x) = \frac{1}{1+\exp\left[\frac{-(x-x_{th})}{\Delta x}\right]}, \; x: \; P, \; E, \; I, ED \tag{1}$$

$$\Delta\widetilde{x} = \frac{\Delta x}{x_{th}} \tag{2}$$

where the x represents the evaluated laser parameter such as peak power, P; pulse energy, E; and peak-power intensity (peak power per unit area), I; and pulse energy density (pulse energy per unit area), ED. The solid red line shows the fitting curve given by (1) in Figure 3b,c,e,f. According to the numerical fitting, the P_{th} corresponding to 50% breakdown probability was 0.972 MW. In other words, the I_{th} was determined to be 0.63 TW/cm^2. In addition, the ΔP and $\Delta\widetilde{P}$ was found to be 44 kW and 0.045, respectively.

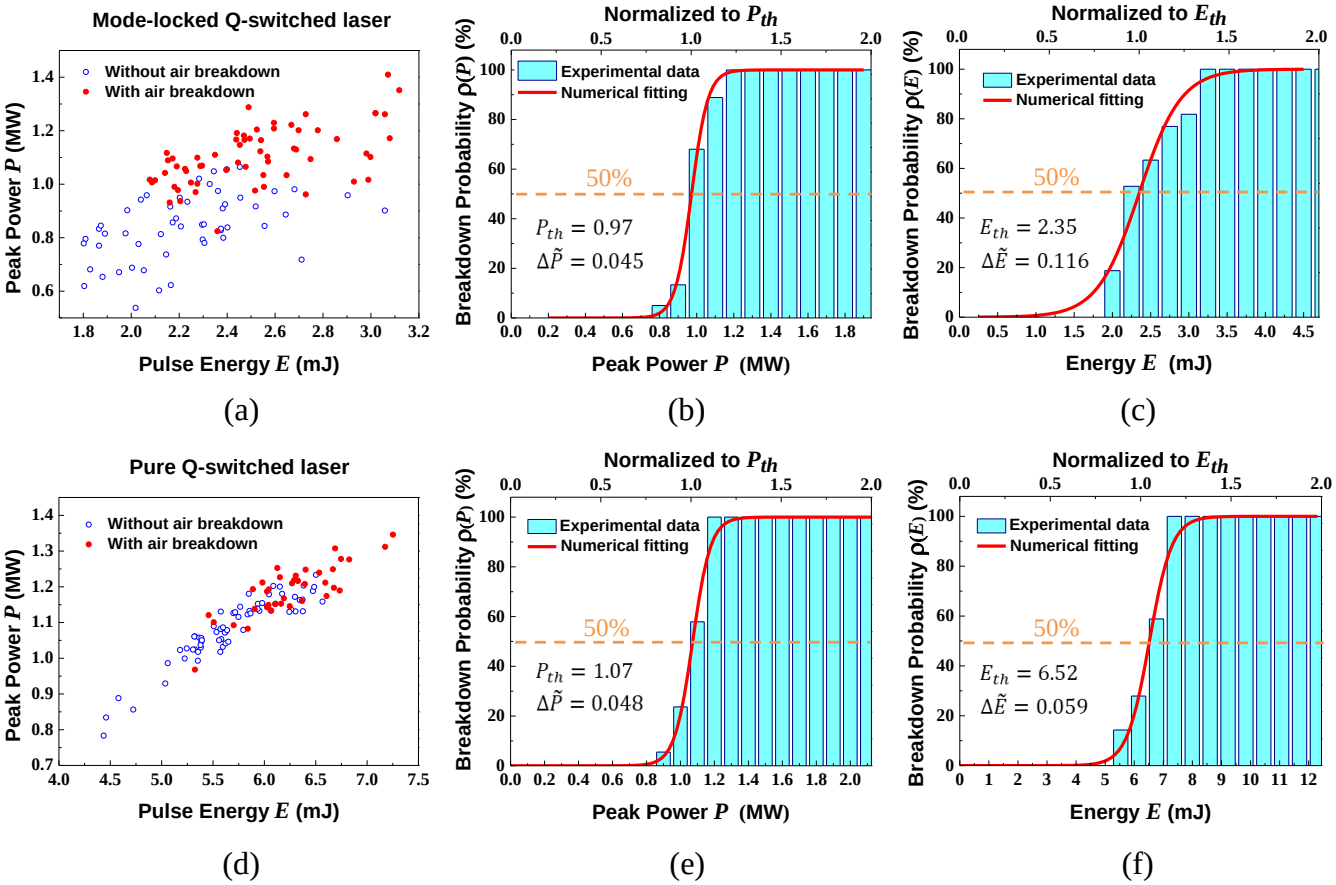

Figure 3. (**a**,**d**) Relation of the success of air breakdown to the laser pulse energy and peak power with mode-locked Q-switched laser and pure Q-switched laser, respectively. (**b**,**c**,**e**,**f**) Histogram and fitting curve (red line) of the breakdown probability versus the pulse peak power and energy in (**a**,**d**), respectively.

The histogram of breakdown probability with respect to the pulse energy was performed in Figure 3c. According to the numerical fitting, the E_{th}, ED_{th}, ΔE, and $\Delta\widetilde{E}$ was found to be 2.35 mJ, 1.53 kJ/cm^2, 0.273 mJ, and 0.116, respectively. The $\Delta\widetilde{E}$ was significantly larger than the $\Delta\widetilde{P}$, which indicated the peak power was the principal threshold condition and consistent with the qualitative observation.

In order to verify that the ML-QS pulse has a lower energy threshold than pure Q-switched (p-QS) pulse, the typical p-QS pulses with 7-ns duration were generated by adding a feedback mirror to inject a weak etalon effect. The p-QS laser pulse had almost the same beam quality and pulse width as the ML-QS laser pulses. Figure 3d–f show the experimental results and statistic analysis of air breakdown with p-QS pulses. According to the numerical fitting, the P_{th}, I_{th}, ΔP, and $\Delta\widetilde{P}$ was found to be 1.07 MW, 0.70 TW / cm^2, 52 kW, and 0.048, respectively. The E_{th}, ED_{th}, ΔE, and $\Delta\widetilde{E}$ was found to be 6.52 mJ, 4.23 kJ/cm^2, 0.382 mJ, and 0.059, respectively. The results demonstrate that the threshold peak power of ML-QS pulse was similar, only 0.91 times lower than the p-QS pulse. Moreover, the reason might be that the transverse mode quality of the ML-QS laser was still slightly better than the p-QS laser with feedback injection. However, the threshold energy of the ML-QS pulse was significantly 0.36 times lower than the p-QS pulse.

As stated above, the peak-power intensity was approved to be a more suitable condition than the energy density for a Q-switched laser to determine the air breakdown threshold. For p-QS pulses, the $\Delta\widetilde{P}$ of 0.048 is smaller than the $\Delta\widetilde{E}$ of 0.059. Because there is no big difference in pulse shape, defining the threshold value based on the peak power is slightly better than energy. However, through the qualitative and quantitative results of

ML-QS pulses, we confirm that the peak-power intensity is the critical condition rather than the energy density. Furthermore, the statistic method can explicitly evaluate the threshold value and threshold width which is related to the peak power stability of the laser source and the breakdown environment.

Reference [20] was chosen for comparison with previous literature works due to its similar breakdown conditions. The breakdown threshold energy was 13.4 mJ by use of the 1064-nm 6.5-ns p-QS pulses. With an estimated beam radius of 9 μm, the ED_{th} would be 5.1 kJ/cm^2, close to the ED_{th} of 4.23 kJ/cm^2 for p-QS pulse in this work.

3.3. Temporal Characteristics of Air Breakdown

After determining the air breakdown threshold condition from different pulse shapes, the laser was operated to output modulated pulses with high peak power intensity that can 100% induce plasma signal for studying the temporal dynamics. Figure 4a depicts the temporal characteristics for the incident pulse, residual pulse, and the radiation of induced plasma after carefully calibrating time delay from the optical path difference. The temporal profiles of the incident and residual pulse reveal that the air molecules absorb only partial energy from the excitation pulse at the initial stage before the plasma is triggered. When the power intensity exceeds the threshold for air breakdown; however, most of the energy for the excitation pulse is depleted to build up the radiation of plasma with a rising time of about 2 ns. In addition, when the decaying instantaneous power of the excitation pulse is insufficient to sustain the buildup of plasma, plasma radiation begins to decay with a decaying time of a few tens of nanoseconds. Intriguingly, there were small peaks on the radiation pulse shape of induced plasma, corresponding to the mode-locked modulation subpulses of the incident laser pulse. It implied that the ionization process and correspondent plasma core density might be modulated rapidly, too. However, due to the long decay time of radiation, the fast dynamics cannot be seen through radiation directly. The fast dynamics was observed by the self-scattering method in the coming section.

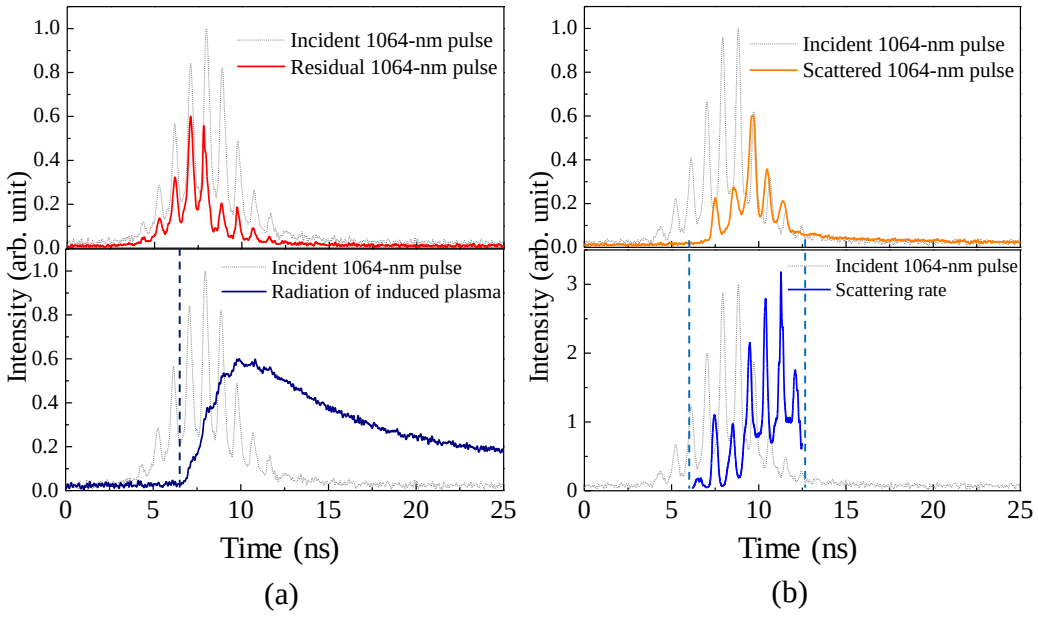

Figure 4. (**a**) Temporal characteristics for the 1064-nm incident pulse, 1064-nm residual pulse, white-light radiation of induced plasma. (**b**) Temporal characteristics for the 1064-nm incident pulse, the 1064-nm scattered pulse and the calculated scattering rate.

By replacing the HR-1064 nm filter with a band-pass filter at 1064 nm in front of the photodiode—PD2, we found that the 1064 nm pulse laser was scattered by the plasma induced by the laser itself. Here, we called the phenomenon 'self-scattering'. The temporal characteristic of the scattered 1064 nm pulse in the above experiment was illustrated in the

upper part of Figure 4b. Dividing the temporal trace of scattered pulse to the incident pulse, we defined the above temporal result as scattering rate, which was shown in the lower part of Figure 4b. With the self-scattering method, the time-dependent scattering ability of induced plasma was obtained without additional probe light. Notice that when the signal of the scattered pulse was small, the calculated result of the scattering rate showed plenty of noise, which was ignored in the lower part of Figure 4b.

Furthermore, the start-up time of scattering rate was matched the third subpulse that can induce initial breakdown with the power exceeding threshold power, and was 0.25 ns before the plasma emission observed. It implies that the self-scattering method could be useful for studying the plasma formation after comparing quantitatively with the method of interferometry, shadowgraphy, or high-speed photography using ns intensified CCD.

Finally, the time-averaged radiation spectrum of the induced plasma was further measured, as shown in Figure 5. The peaks of the experimental spectrum were found to correspond to the excited levels of the gas molecules in the air [36] well. In addition, the envelope of the radiation spectrum is confirmed to be in good consistence with the reported result in previous literature [41].

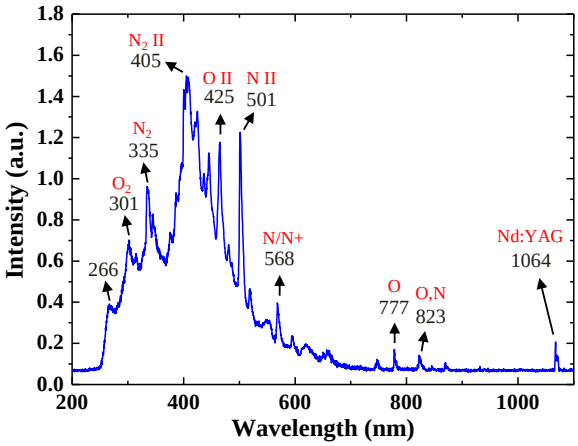

Figure 5. Time-averaged radiation spectrum of the induced plasma in air.

4. Conclusions

In summary, a lamp-pumped Q-switched Nd:YAG laser at 1064 nm with mode-locked modulations has been utilized to explore the threshold of air breakdown. It is feasible to utilize pulse-by-pulse monitoring and the statistic method to precisely determine the breakdown threshold value and threshold width. As shown in the present work, the breakdown threshold was dominated by peak-power intensity. Moreover, the increased peak power by the deep mode-locking modulations can significantly reduce the required pulse energy for laser-induced breakdown.

Furthermore, the radiation of induced plasma rises rapidly while the instantaneous power exceeds the threshold power and displays a decaying time of a few tens of nanoseconds. With the self-scattering method, the time-dependent scattering ability of induced plasma can be obtained without additional probe light.

Author Contributions: Conceptualization, K.-W.S. and P.-H.T.; Validation, C.-H.W., P.-H.W., K.-T.Y. and K.-W.S.; Formal analysis, K.-T.Y., P.-H.T., C.-H.W. and K.-W.S.; Resources, K.-W.S.; Writing—original draft preparation, K.-T.Y. and P.-H.T.; Writing—review and editing, K.-W.S.; Supervision, K.-W.S. All authors have read and agreed to the published version of the manuscript.

Funding: This research received no external funding.

Institutional Review Board Statement: Not applicable.

Informed Consent Statement: Not applicable.

Data Availability Statement: All of the data reported in the paper are presented in the main text.

Conflicts of Interest: The authors declare no conflict of interest.

References

1. Maker, P.D.; Terhune, R.W.; Savage, C.M. Optical third harmonic generation. In Proceedings of the 3rd International Quantum Electronics Conference, Paris, France, 29 May–3 June 1963; Volume 2, pp. 1559–1572.
2. Meyerand, R.G., Jr.; Haught, A.F. Gas breakdown at optical frequencies. *Phys. Rev. Lett.* **1963**, *11*, 401–403. [CrossRef]
3. Panchenko, A.N.; Shulepov, M.A.; Tel'Minov, A.E.; Zakharov, L.A.; Paletsky, A.A.; Bulgakova, N. Pulsed IR laser ablation of organic polymers in air: Shielding effects and plasma pipe formation. *J. Phys. D Appl. Phys.* **2011**, *44*, 385201. [CrossRef]
4. Mon, T.T.; Muhamad, K.F.; Ahmad, A.H.; Mohid, Z. Experimental Micromachining of Silicon with Nd-YAG Laser. *Appl. Mech. Mater.* **2011**, *83*, 244–248. [CrossRef]
5. Ashmore, P.G. *Photochemistry and Reaction Kinetics*; Cambridge University Press: London, UK, 1967.
6. Andersson, P.U.; Holmlid, L. Fusion Generated Fast Particles by Laser Impact on Ultra-Dense Deuterium: Rapid Variation with Laser Intensity. *J. Fusion Energy* **2012**, *31*, 249–256. [CrossRef]
7. Miziolek, A.W.; Palleschi, V.; Schechter, I. *Laser Induced Breakdown Spectroscopy*; Cambridge University Press: Cambridge, UK, 2006.
8. Pavel, N.; Tsunekane, M.; Taira, T. Composite, all-ceramics, high-peak power Nd:YAG/Cr(4+):YAG monolithic micro-laser with multiple-beam output for engine ignition. *Opt. Express* **2011**, *19*, 9378–9384. [CrossRef]
9. Taira, T. Domain-controlled laser ceramics toward Giant Micro-photonics [Invited]. *Opt. Mater. Express* **2011**, *1*, 1040–1050. [CrossRef]
10. Chen, R.C.C.; Yu, Y.T.; Su, K.W.; Chen, J.F.; Chen, Y.F. Exploration of water jet generated by Q-switched laser induced water breakdown with different depths beneath a flat free surface. *Opt. Express* **2013**, *21*, 445–453. [CrossRef]
11. Raizer, Y.P. *Gas Discharge Physics*; Springer Science and Business Media LLC: New York, NY, USA, 1991; p. 7.
12. Kroll, N.; Watson, K.M. Theoretical Study of Ionization of Air by Intense Laser Pulses. *Phys. Rev. A* **1972**, *5*, 1883–1905. [CrossRef]
13. Chan, C.H.; Moody, C.D.; McKnight, W.B. Significant loss mechanisms in gas breakdown at 10.6 μm. *J. Appl. Phys.* **1973**, *44*, 1179. [CrossRef]
14. Amoruso, S.; Bruzzese, R.; Spinelli, N.; Velotta, R. For laser ablation. *J. Phys. B At. Mol. Opt. Phys.* **1999**, *32*, R131. [CrossRef]
15. Kaselouris, E.; Nikolos, I.K.; Orphanos, Y.; Bakarezos, E.; Papadogiannis, N.A.; Tatarakis, M.; Dimitriou, V. For ns laser matter interaction. *J. Multiscale Model.* **2013**, *5*, 1330001. [CrossRef]
16. Polynkin, P.; Moloney, J.V. Optical breakdown of air triggered by femtosecond laser filaments. *Appl. Phys. Lett.* **2011**, *99*, 151103. [CrossRef]
17. Shneider, M.N.; Miles, R.B. Laser induced avalanche ionization in gases or gas mixtures with resonantly enhanced multiphoton ionization or femtosecond laser pulse pre-ionization. *Phys. Plasmas* **2012**, *19*, 083508. [CrossRef]
18. Thiyagarajan, M.; Thompson, S. Optical breakdown threshold investigation of 1064 nm laser induced air plasmas. *J. Appl. Phys.* **2012**, *111*, 73302. [CrossRef]
19. Brieschenk, S.; Kleine, H.; O'Byrne, S. On the measurement of laser-induced plasma breakdown thresholds. *J. Appl. Phys.* **2013**, *114*, 093101. [CrossRef]
20. Chen, Y.-L.; Lewis, J.; Parigger, C. Spatial and temporal profiles of pulsed laser-induced air plasma emissions. *J. Quant. Spectrosc. Radiat. Transf.* **2000**, *67*, 91–103. [CrossRef]
21. McMillian, M.H.; Woodruff, S.D.; Richardson, S.W.; McIntyre, D. Laser Spark Ignition: Laser Development and Engine Testing. In Proceedings of the ASME 2004 Internal Combustion Engine Division Fall Technical Conference, American Society of Mechanical Engineers. Long Beach, CA, USA, 24–27 October 2004; pp. 823–832.
22. Phuoc, T.X. Laser spark ignition: Experimental determination of laser-induced breakdown thresholds of combustion gases. *Opt. Commun.* **2000**, *175*, 419–423. [CrossRef]
23. Nishihara, M.; Freund, J.B.; Glumac, N.G.; Elliott, G.S. Influence of mode-beating pulse on laser-induced plasma. *J. Phys. D Appl. Phys.* **2018**, *51*, 135601. [CrossRef]
24. Tambay, R.; Thareja, R.K. Laser-induced breakdown studies of laboratory air at 0.266, 0.355, 0.532, and 1.06 μm. *J. Appl. Phys.* **1991**, *70*, 2890–2892. [CrossRef]
25. Du, D.; Liu, X.; Korn, G.; Squier, J.; Mourou, G. Laser-induced breakdown by impact ionization in SiO2with pulse widths from 7 ns to 150 fs. *Appl. Phys. Lett.* **1994**, *64*, 3071–3073. [CrossRef]
26. Chýlek, P.; Jarzembski, M.A.; Srivastava, V.; Pinnick, R.G. Pressure dependence of the laser-induced breakdown thresholds of gases and droplets. *Appl. Opt.* **1990**, *29*, 2303–2306. [CrossRef]
27. Armstrong, R.A.; Lucht, R.A.; Rawlins, W.T. Spectroscopic investigation of laser-initiated low-pressure plasmas in atmospheric gases. *Appl. Opt.* **1983**, *22*, 1573–1577. [CrossRef]
28. Bärwinkel, M.; Lorenz, S.; Stäglich, R.; Brüggemann, D. Influence of focal point properties on energy transfer and plasma evolution during laser ignition process with a passively q-switched laser. *Opt. Express* **2016**, *24*, 15189. [CrossRef]
29. Lim, H.H.; Taira, T. Sub-nanosecond laser induced air-breakdown with giant-pulse duration tuned Nd:YAG ceramic micro-laser by cavity-length control. *Opt. Express* **2017**, *25*, 6302–6310. [CrossRef]
30. Ireland, C.L.M. Gas breakdown by single, similar 40 ps–50 ns, 1.06 μm laser pulses. *J. Phys. D Appl. Phys.* **1974**, *7*, L179–L183. [CrossRef]
31. Phuoc, T.X. Laser-induced spark ignition fundamental and applications. *Opt. Lasers Eng.* **2006**, *44*, 351–397. [CrossRef]

32. Cho, C.Y.; Huang, Y.P.; Huang, Y.J.; Chen, Y.C.; Su, K.W.; Chen, Y.F. Compact high-pulse-energy passively Q-switched Nd:YLF laser with an ultra-low-magnification unstable resonator: Application for efficient optical parametric oscillator. *Opt. Express* **2013**, *21*, 1489–1495. [CrossRef]
33. Liang, H.C.; Huang, Y.J.; Huang, W.C.; Su, K.W.; Chen, Y.F. High-power, diode-end-pumped, multigigahertz self-mode-locked Nd:YVO4 laser at 1342 nm. *Opt. Lett.* **2009**, *35*, 4–6. [CrossRef]
34. Huang, Y.P.; Cho, C.Y.; Huang, Y.J. Efficient high-energy pulse generation from a diode-side-pumped passively Q-switched Nd:YAG laser and application for optical parametric oscillator. *Laser Phys. Lett.* **2014**, *11*, 095001. [CrossRef]
35. Han, C.; Zhao, S.; Li, D.; Li, G.; Yang, K.; Zhang, G.; Cheng, K. Optimization of the pulse-width of diode-pumped passively Q-switched mode-locked c-cut Nd:GdVO4 laser with a GaAs saturable absorber. *Appl. Opt.* **2011**, *50*, 5970–5976. [CrossRef] [PubMed]
36. Chen, Y.-F.; Huang, K.F.; Tsai, S.W.; Lan, Y.P.; Wang, S.C.; Chen, J. Simultaneous Mode Locking in a Diode-Pumped Passively Q-Switched Nd:YVO(4) Laser with a GaAs Saturable Absorber. *Appl. Opt.* **2001**, *40*, 6038–6041. [CrossRef] [PubMed]
37. Puliafito, C.A.; Stoinert, R.F. Short-pulsed Nd:YAG laser microsurgery of the eye: Biophysical considerations. *IEEE J. Quantum Electron.* **1984**, *20*, 1442–1448. [CrossRef]
38. Psaltis, D.; Quake, S.R.; Yang, C. Developing optofluidic technology through the fusion of microfluidics and optics. *Nat. Cell Biol.* **2006**, *442*, 381–386. [CrossRef] [PubMed]
39. Machala, Z.; Janda, M.; Hensel, K.; Jedlovský, I.; Leštinská, L.; Foltin, V.; Martišovitš, V.; Morvová, M. Emission spectroscopy of atmospheric pressure plasmas for bio-medical and environmental applications. *J. Mol. Spectrosc.* **2007**, *243*, 194–201. [CrossRef]
40. Krausz, F.; Fermann, M.; Brabec, T.; Curley, P.; Hofer, M.; Ober, M.; Wintner, E.; Schmidt, A.; Spielmann, C. Femtosecond solid-state lasers. *IEEE J. Quantum Electron.* **1992**, *28*, 2097–2122. [CrossRef]
41. Borghese, A.; Merola, S.S. Time-resolved spectral and spatial description of laser-induced breakdown in air as a pulsed, bright, and broadband ultraviolet-visible light source. *Appl. Opt.* **1998**, *37*, 3977–3983. [CrossRef]